REVISING TESTING OF COMPOSITE PRECURSORS – A NEW FRAMEWORK FOR DATA CAPTURE IN COMPLEX MULTI-MATERIAL SYSTEMS

Anatoly Koptelov[1*], Jonathan P.-H. Belnoue[1], Ioannis Georgilas[2], Stephen R. Hallett[1], Dmitry S. Ivanov[1]

[1] Bristol Composites Institute, University of Bristol, Bristol, BS8 1TR, United Kingdom,

[2] University of Bath, Bath, BA2 7AY, United Kingdom

*Corresponding author. E-mail address: anatoly.koptelov@bristol.ac.uk

ABSTRACT:

Any composite manufacturing method requires an application of a carefully designed consolidation process to ensure the suppression of voids in the laminate, establish bonding in laminate layers and prevent dimensional or fibre-path defects. The optimisation of consolidation processes relies on the characterisation of the composite precursors' deformability. There are multiple mechanisms occurring in consolidation and various experimental programmes have been suggested in the literature to describe these mechanisms and deduce relevant material properties. The selection of a testing methodology often relies on an initial hypothesis or prior knowledge regarding the deformation modes. This may be a source of significant errors. This paper poses questions on the testing rationales, on subjectivity in material testing and on how data-rich programmes should be designed. Two approaches are suggested – the first one is a real-time adaptive testing strategy that enables a "conversation with the material" – flexible autonomous steering of a testing programme reacting on the obtained output. This framework focuses on the identification of the underlying physical mechanisms rather than material properties identification in a rightly or wrongly assumed flow mode. The second approach examines favourable combinations of tests to maximise information obtained whilst minimising the amount of testing. The obtained results highlight a way forward in terms of rethinking experiments for materials used in manufacturing and beyond.

Keywords: C. Process Modelling, D. Process monitoring, E. Consolidation, E. Resin flow

1. Introduction

The consolidation of composite precursors is a quality-critical process in the manufacture of composites. It is essential in forming of thermoplastic components, debulking/autoclaving of prepregs, thermoforming of textile preforms prior to liquid moulding, etc. Deformability of composite precursors defines their susceptibility to defects [1], their compliance with dimensional tolerances [2], and the occurrence of shape

distortions [3]. Material response in consolidation arises from a complex interaction of various deformation mechanisms (i.e. the internal or percolation flow of resin [4], flow of fibrous suspensions [5], densification of reinforcement [6,7], relative movement of plies [8], and others). Different forms of these mechanisms take place at different structural scales and often occur in parallel or exhibit transition from one state to another. For instance, shear flow of an incompressible suspension can occur at the scale of resin bridges connecting isolated plies [9], of tapes deposited in automatic fibre deposition (AFP) processes [10], of individual yarns in dry fabric [11], of broad good prepreg plies [12], or even of entire component [13]. Percolation flow may occur within partially impregnated fibre bundles [14], from fibre bundles to inter-yarn/tape space [15] and/or from plies to external bleeders [16]. It is essential to have a comprehensive understanding of all these processes to predict the evolution of precursors throughout all the stages of composite processing and assess the final architecture/properties of the composite structure. Each of these mechanisms can be described by material models with various formulations involving large number of constants. There is a vast variety of different physical models translating material behaviour into explicit viscoelastic load-displacement response. The identification of these flow modes and associated constants is key to precursor characterisation. Material characterisation tests are drastically different depending on which mechanism is assumed to be prevailing. There is no standardised testing strategy that would be equally suitable for all the observed deformation/flow mechanisms. In simple cases, isolated experiments with material components (e.g. compaction of dry reinforcement, rheological experiments on pure resin [17] or resin suspension [18]) can provide all the required input to describe the material behaviour. However, this is only the case when the model can precisely capture how individual components interact in the system. Often, reality suggests much more complex interaction mechanisms with no clear route to test constituents separately. For instance, the behaviour of dry reinforcement and the same reinforcement in an impregnated preform will behave differently due to lubrication [19]. Other examples include transitional behaviours where different flow processes occur at different stages of the processes [12]. In these cases, the testing programmes require inverse property calculation procedures, and depend on the model and the initial hypothesis made by the experimenter. Examples available the in literature include the monotonic compression testing at various rates [20], relaxation and creep tests [21,22], ramp-dwell programmes to separate viscous and elastic contributions of fibrous and resin components [23], ramp-dwell programme motivated by the need to cover wider range of

strain-rates [24], etc. Material constants can then be identified based on an optimisation procedure which attempts to minimise the deviation of the model predictions from the measured experimental data.

A potentially dangerous trap is that available experimental data are often limited as material testing is both complicated and time consuming. Hence, the information obtained in these tests may appear to be deficient and may not reveal all the underlying processes. In this case, property identification may provide a seemingly good fit irrespective of which mechanisms is presumed to happen. However, it does not mean that such model represents the physical reality, and it can often fail to adequately represent a wider set of experimental data. This sets a fundamental dilemma, as the material behaviour (i.e., the model selected) needs to be decided prior to conducting the tests, which introduces a strong subjective element. There is, therefore, a need in a new testing methodology that is capable to identify the deformation mechanisms as well as the relevant material properties. This methodology should be able to check different hypothesis on the deformation mechanisms and autonomously design a testing programs based on the measured behaviour of the material. This methodology should also lead to reduced number of experiments while making sure that the obtained data is representative and sufficiently captures all the main features of the material behaviour.

This paper presents a framework for such a novel testing methodology. It is designed as an active system where the decision about testing programme in terms of load and load rate is taken in real time and driven by pursuit of identification of model physics. It is not bound by any predefined assumptions about material's behaviour. Therefore, there is no bias towards any preferred consolidation model. In that case an algorithm is not limited by previous testing experience and is adaptable to any material chosen for testing. The system's algorithm is set to track characteristic patterns in a material's behaviour relevant to existing consolidation models. Based on feedback a consolidation sensor framework formulates a load schedule for the subsequent load step of the test. The system deploys a library of material models and checks the hypothesis that each of these models uses to describe the deformation. The system optimises the loading trajectory for the following step in the test in such a way to distinguish the most capable candidate among considered models.

In this work the reliability of such methodology is checked in a virtual exercise. The suggested testing framework, implemented as an interactive algorithm, is set to identify the right mechanisms and extract parameters of a material model hidden in a pre-coded module, which simulates a real material response. The paper examines the capability of such a framework to identify the underlying flow mechanisms and sets

relevant test problems. The second part of the paper addresses the behaviour of an actual material with the purpose of examining optimum testing regimes. The material used for characterisation is well examined in previous studies [2,12,25] and known to exhibit complex transitional behaviour. In the following, "optimum" is defined in the sense of a minimum number of tests containing enough information to define the material properties. This testing explores what are the most data-rich testing programmes for some of the characteristic flow mechanisms.

2. Model identification: criteria for model performance

When a unidirectional prepreg tape is compacted between two rigid parallel plates, the application of pressure leads to the build-up of a pressure gradient within the material. This, in turns, induces a resin flow and the deformation of the tape. In this study, we will consider a class of consolidation problems which can be condensed to ordinary differential equations that relate the applied pressure to the change in thickness and thickness rate. This is done using simplifying assumptions and explicit integration of the mass balance, the constitutive and the equilibrium equations. A wide number of relevant consolidation problems can be reduced in this way. This includes the incompressible shear flow of Newtonian and non-Newtonian suspensions under different (tool-material) boundary conditions and the percolation (also refer to as bleeding) flow of impregnated fibrous networks. The general form of the resulting mathematical equation can be written as:

$$\frac{dh}{dt} = F(t,h) \cdot Q(h) \tag{1}$$

where *F(t, h)* is a function containing an evolution of applied pressure with time *t*, *h* is the thickness, $\frac{dh}{dt}$ is the thickness rate, and *Q(h)* is a function of the material parameters. Characteristic models used in this study are summarised in Table 1 (The table also gives abbreviations for each model that will be used in further discussions). The main feature of the proposed framework is that it deploys physical models as the candidates for the library. The models of squeezing or percolation flow are initially formulated for a point in a three-dimensional space and present constitutive equations, mass balance, and equilibrium equations [26]. They are complemented with boundary conditions assuming a certain interaction of the material with loading system. These equations are then integrated under simplifying assumptions to get a one-dimensional pressure-thickness-thickness rate response.

The properties of the laminate are defined by the flow and deformation characteristics of the individual plies. The models deployed in the library are used to deduce the properties of a unidirectional ply and not the effective properties of the laminate. It is essential to emphasize that the considered models assume a certain preferential direction of the resin flow. This assumption is valid as it applies to the tape and not to effective/average sample properties. For instance, the shear flow model suggests that the flow in compaction occurs only in the transverse direction, whereas the flow in the longitudinal direction can be neglected. The percolation model assumes that permeability in one direction is much greater than permeability in the other direction and hence the flow in the other direction can be neglected. The simplifying assumptions allow in some cases to condense the full 3D formulation to a 2D problem without compromising the physical meaning of the studied flow mechanism. Once the pressure-thickness-thickness rate response is identified, all the models in the library can be used to predict full 3D states – including transverse deformations or amount of resin bled through the fibre network [27, 28]. This is fundamentally important when trying to assess not only the thickness evolution but also the process occurring at local scales – e.g. closure of the gaps between the deposited tapes or pressure build-up in resin to assess void suppression. It was shown that the proposed simplifying hypotheses in application to IM7/8552 and IMA/M21 prepregs [1], [2], [12], [24], [26], [27] yield excellent modelling predictive capability, which has been validated with various load cases for laminates and complex composite parts.

The library of structural models is complemented with the DefGen ProToCoL (**Pro**cessing **To**ols for **Co**mposite **L**aminates) model [26,28,29]. This model was developed to describe prepregs with a large range of viscosities at different temperatures. It has characteristic features of both shear and percolation flows. For example, it explicitly links the thickness evolution of a prepreg stack to the initial width and thickness of the constitutive plies within the stack (which is typical for shear flows) and, at the same time, converges to a compaction limit under compression (which is usually related to bleeding flows). The important feature of this model is that both flow mechanisms co-exist, which agrees with the experimental results. This is made possible through the implementation of a transition between flows described as an instant event. This transition from a squeezing to a bleeding flow is triggered when shear deformation at tape edges reaches a critical value. During deformation, the upper fibres move towards the fibres below, thus squeezing the resin in the transverse direction. Currently, when shear deformation reaches its critical value (deformation at locking)

the flow direction changes. At this stage resin bleeds along the fibres (mathematically described as squeezing flow along fibre direction), which is one of the key features of a percolation flow. Hence the model presents a good challenge for testing the framework.

The material constants in equations presented in Table 1 include the viscosity of resin and resin suspensions, the constants describing the evolution of viscosity as functions of shear rate, material constants for the permeability of the fibre network and their dependence on fibre volume fraction, and the constants needed to describe the fibre bed elastic response. As a result, the differential equations contain several material constants that need to be determined holistically to match available experimental data as closely as possible. All these different models not only predict the difference in how, for instance, an impregnated material tape would react to an applied load but also would indicate very different outcome in terms of the width change of the tape, fibre volume fraction, resin pressure distribution, and the uniformity of the deformations within the tape. Consequently, this may lead to very different outcomes in terms of closure of gaps between AFP deposited tapes with suspension or pure resin and follow-up wrinkle occurrence [30]. Investigating the mechanisms occurring at mm-scale would require deep insight on structural deformations such as high-resolution microscopy, CT examinations. On the other hand, it seems plausible that these features may be determined by the difference in mechanical response.

The property identification problem is equivalent to the data regression in the space of thickness rate, thickness, and pressure. The model and property identification procedure can be assessed by examining (a) the quality of the fit for a training set, *i.e.*, the experimental data used to identify material constants and (b) the quality of the fit for an independent validation set of experiments. Low value of the regression error between model's prediction and an experimental data used for training is not enough to safely assume that characterisation was carried out successfully [31]. The discrepancy between the fit in training and validation sets may point at either the deficiency of the training set, the inability of fitting procedure to find global maximum in the space of material parameters, or inadequacy of examined model.

To illustrate it more thoroughly, two different cases of a flawed characterisation are provided below. The experimental data is simulated based on one of the models from the library with an added noise. The experimental data are calculated in response to applied pressure schedule. A set of candidate models from the

library, labelled as models A, B and C, are initialised for material characterisation within training "experimental data" in a training loading set (Figure 1.a).

Upon full material properties identification, these models are trialled against another batch of "experimental data" within a validation set (Figure 1.b). The training schedule is relatively simple and consists of one pressure ramp followed up by dwell at a constant pressure level. The validation test program is more complex and consists of several ramp-dwell stages. The characterisation is considered successful if a trained model is able to adapt to a changing load input and to describe the validation batch of 'experimental data'.

In the first identification problem, two different models (model A = DefGen ProToCoL model, model B = squeezing non-Newtonian flow (nvfs_pow)), drawn as green and red curves respectively in Figure 1.c, are fitted against a training data set. Both models exhibit a very similar agreement with the "experimental data" – Figure 1.c. The simulator of experimental data is based on the DefGen ProToCoL model with added noise, which is the same as one of the candidate models. As illustrated in Figure 1.d, after being exposed to a more complex validation loading program, the model B completely fails to output a feasible prediction of the material's behaviour. However, at the training stage, this same model B (that is different from the model used to simulate an experiment) was able to better fit the simulated experimental response. This perfectly illustrates the importance of a validation check. This is a typical example of model's overfitting and that was reported by numbers of researchers in various fields [32], [33]. Governing equations of high-performance consolidation models may contain complex over-parameterised terms and are able to fit any given data set [34], which may lead to overfitting of the training input sets [35]. In such a case, the underlying patterns and relationships of the experimental data are not captured by the algorithm. Instead, dependencies only specific to the training case are taken into account, which are not relevant for the whole range of possible load cases. Consequently, a model is likely to provide a wrong prediction for a different history of pressure evolution [36].

Another possible challenge is an encounter of a local minimum of an objective function. If a chosen consolidation model is a strong non-convex function, it may exhibit multiple local minima. In this case the result of a characterisation largely depends on a starting vector of material parameters [37]. Several local minima of a target function result in a more than one set of parameter values which fit the training data equally well [38]. Therefore, if a starting vector is next to a local minimum of an objective function, an optimiser will not converge to the correct material parameters [39]. This will cause a disrupted model's

prediction for an input different from training data. An illustration of that scenario is shown in Figure 1.e. Here the exact same model C is used twice, but with different sets of initial values for parameters definition. The experimental data is an instance of the same model C. Yet again, both are shown to find the good match with training set. However, only the model with a more appropriate set of initial parameters converges to a global optimum. Therefore, it is able to adapt to a changing load program and to adequately predict material's response (see Figure 1.f.). Completeness of both the training and validation experiments needs to be carefully examined. Tests that lack structural information may lead to misleading outcomes in prediction of the correct flow mechanism. An optimum programme for both may appear to be dependent on the material behaviour. Therefore, there is a clear need in a more sophisticated testing algorithm (considered in the next section) or a more thorough examination of testing procedure (considered in the second part of the paper).

3 Adaptive testing framework

3.1 Conceptual design

The adaptable testing programme suggested below aims at identifying flow mechanism as a result of a continuous material's compaction response and at an analysis of the obtained data in real time. The primary driver for such an algorithm is not to determine the material properties per se (though this is also achieved as a by-product of the process), but to select the right flow model. For a start, we will assume that the compacted material can be adequately described by one of the consolidation models from a pre-defined library, but there is no prior knowledge about what model should be chosen. The library contains models in the form of ordinary differential equations (such as shown in Table 1).

The pressure-controlled loading programme is fragmented into a sequence of steps. There is a fixed time defined for each of these steps. At the end of each step the load can be ramped (faster, slower or in ramp-dwell fashion), or the material may be allowed to relax under constant load. No unloading is considered at this stage though this may be an interesting development particularly when models with plastic response are added to the library (see Figure 2a). The decision of what needs to be done for a particular load stage is dictated by the framework for all the stages except the very initial step. At the start of the loading a predefined compression load is applied since there has not been any experimental data received at this point.

The output of this testing is an evolution of the sample thickness throughout all loading stages. At each stage of an experiment the consolidation sensor starts challenging every model from the library to determine its

ability to characterise the material. This is done by conducting a nonlinear regression analysis of a candidate model, in which the algorithm finds the best combination of material parameters that allows a candidate model to fit the experimental data as accurately as possible. Therefore, after reviewing the consolidation library, a set of material parameters corresponding to a particular flow model is retrieved. It is now possible to predict the material's feedback to a possible load schedule change in further load steps of the test in accordance with a chosen consolidation model. Moreover, fit quality provides some preliminary ranking of the models. After reviewing the results from the current stage, the two most capable candidate models are selected. The selection is based on the value of root mean square error between the models' feedback and actual data. These two candidates are then passed to the load schedule definition module. Possible load schedule scenarios are selected by picking the load option which maximises the difference in prediction between the two best candidate models. This way, the resulting testing program is designed in a way, which allows to distinguish between best performing consolidation models most efficiently and to reduce the uncertainty on the material's deformation mechanism to a minimum. The following stage is to submit a newly designed load schedule as an input to the testing rig for the next load step. The whole process is then repeated until the testing is over. The detailed algorithm of the framework is illustrated in Figure 2b. The framework was implemented in the Python programming language environment [40] using the nonlinear optimization package *lmfit* [41].

3.2. Implementation of the framework

Since the consolidation models in the library are represented in a form of differential equations, the framework has to solve a chosen differential equation to retrieve thickness over time data. Solving an equation requires an input of a timespan array $[t_0 \quad t_1 \quad \cdots \quad t_n]$ along with the corresponding array of force values $[F_0 \quad F_1 \quad \cdots \quad F_n]$. Additionally, a set of material parameters for a picked consolidation model must be provided. After successful integration on a defined time interval, a resulting thickness array $[h_0 \quad h_1 \quad \cdots \quad h_n]$ is output. The model's governing equation involves a function $F(t, h)$, which represents an applied compression load. It is a time-dependent function. This feature introduces additional complexity for the solver. Due to the time-dependent component, it is, now, not possible to integrate the whole timespan of the test using standard solver tools, hence, the framework solves the differential equation in a step-by-step mode by sequentially integrating data on the $[t_{i-1} \quad t_i]$ intervals. A solution on an interval $[t_{i-1} \quad t_i]$ satisfies

the prescribed boundary condition $h(t_{i-1}) = h_{i-1}$. The thickness value h_{i-1} is recovered from a previous interval $[t_{i-2} \quad t_{i-1}]$ integration and updated at each step. Thus, it is possible to take into the account time-dependant force function by updating its value at each time interval.

3.3. Parameters extraction

A comprehensive parameters extraction procedure is required to retrieve true values (i.e. global minimum) of the identified material parameters for a chosen model. An extra level of complexity is added due to the real-time nature of the experimentation. Interim results analysis takes place while a characterisation test is still running. For this reason, the framework's execution time must be reduced to a minimum, as opposed to standard postprocessing procedures where computational promptness is less critical.

The essence of the nonlinear regression process is to minimise an objective function by varying its parameters. An objective function is the cumulative difference between experimental compaction data and the thickness prediction of the candidate model. As illustrated in Section 2 of this paper, one of the main challenges for a regression algorithm is to avoid sticking in a local minimum. Hence, it is of the utmost importance to pick reasonable initial values for material constants in optimisation and do it without sacrificing computational speed. For this reason, a two-stage optimisation procedure is utilised within the proposed framework.

The flowchart of this procedure is presented in Figure 3. At the initial stage, the objective function is minimised over a given range of parameter values by an exhaustive search method, hereinafter referred to as a brute force method. The primary goal is to establish a feasible set of initial values for material constants which are then used for further minimisation. To achieve that, an objective function is evaluated at each point of a multidimensional grid of possible parameter values. In general, the brute force method is inefficient and takes a long time to execute. The total number of objective function evaluations equals n^d, where n is the number of parameters and d is the density of the grid. Therefore, finding a global minimum for complex models with three or more material parameters would require an enormous amount of computational time, which contradicts the purpose of real-time processing. Hence, an objective function is minimised over a grid with a coarse spacing. The best result is then used as a starting point at the second stage of the parameters extraction where it is possible to select a nonlinear optimisation method of choice. The two main approaches used are the Nelder-Mead [42] and the nonlinear least squares [43] methods. Upon completion of the routine,

an optimal parameter set for each candidate model is retrieved. The parameters extraction routine is repeated at each load step of the test. It is possible to use a parameter set from a previous load step as a starting point for the current one. In this case, the brute force stage can be omitted which speeds up the whole process. Since optimisation methods at the second stage are not global, there is still a possibility of converging to a local minimum. In that case the density of the grid used at the brute force stage can be increased to provide a more favourable set of starting parameters. There are a number of global optimisation approaches, which, by definition, are independent of the parameters' initial values and always converge to a global minimum e.g. Basin-hopping method [44], differential evolution [45]. However, due to the high computational cost they are not applicable in a real-time experimentation with tight time constraints.

As stated before, the framework's processing speed is of prime importance. An important factor of processing the results is that the analysis of each candidate model is independent of each other. On this account, it becomes possible to significantly speed up the overall parameters extraction routine by processing each candidate model from the consolidation library in a concurrent manner. By leveraging all available CPU cores, tasks for execution can be submitted as separate processes [46]. The framework automatically manages a pool of candidates to be processed and assigns available cores to perform the parameters extraction. Therefore, if the number of CPU cores (including virtual cores) in the machine is more or equal to the number of models in the library, the total execution time is limited by the most complex and slowest candidate model. One characterisation test may not reveal all features of the material behaviour. In this case more testing schedules with different load levels and load rates have to be explored. Although the framework is designed to operate on the fly, it is possible to apply the parameters extraction module to a conventional experiment for data postprocessing after the test is done. A more thorough optimisation can be conducted as the time constraints are lifted. This includes a denser brute optimisation and larger volumes of training data. It is possible to expand the studied data by considering joined compaction datasets from several experiments within a single parameters extraction iteration. It allows the candidate model to take into account experimental programmes with various loading history and to be trained directly on the corresponding material's feedback. The parameters extraction routine's source code is available at https://accis.github.io/DefGenParFit.

3.4 Virtual testing

To validate the predictive capacity of the suggested framework, virtual tests have been performed. Similar to the example in Section 2 of this paper, the material behaviour is simulated by an instance of one of the models in the library with added noise representing uncertainty of the experiments. The simulated material response is produced by a virtual module hereinafter referred to as 'BlackBox'. The BlackBox module's routine is presented in Figure 4. Before the start of the experiment, one target model from the library is selected and fully defined by specifying all required parameters. Then, it is placed inside the BlackBox module. The consolidation framework is unaware of what model is hidden inside the BlackBox. The main goal here is to investigate predefined flow mechanism and its parameters by challenging candidates from the library as in a real experiment.

The setup for the virtual exercise replicated the conceptual design for examining real materials shown in Figure 2.b. The only difference is that the interaction between the testing machine and the tested samples is substituted with the BlackBox module, which simulates the behaviour of material in response to the evolving compression programme. Similarly to a universal test machine, the proposed module receives a load program as an input. After the load schedule input is submitted to the BlackBox, a differential equation corresponding to a hidden target model is solved and outputs the evolution of the sample's thickness over time. Then, a noise component is added to the resulting thickness output to introduce an extra challenge for the framework. The main advantage of virtual testing is that the correct material formulation is known; therefore, the framework's performance can be directly assessed by comparing the target model in the BlackBox and the model defined by the testing framework. The success of the current batch of the models is when each of them can be properly detected from live interaction with the "material".

The following example of virtual testing shows a fully defined DefGen ProToCoL model initialised inside the BlackBox module using parameters of Table 2. The test consisted of ten load steps with a duration of 10 seconds per step. Initial ramp-dwell schedule with a maximum amplitude of 30 N was conducted at the start of the test. The maximum possible load change within one load step was set at 30 N. Every model from the library, including the DefGen model, was challenged to fit the BlackBox's output at each load step of the test. Prior to the experiment, initial values of model parameters for the candidate models were set up randomly within defined limits. These were set based on maximum/minimum achievable values of material parameters within a chosen consolidation model.

A visual representation of a virtual testing process is illustrated on Figure 5. Each load step figure consists of three separate graphs. The BlackBox's thickness evolution curve and two best performing candidate models' feedback curves are depicted on the left. There is also an area of the candidates' predicted output for a chosen load within the next load step, which maximises the difference in thickness evolution between them. There is also a noisy output of the BlackBox similar to the example presented in Figure 4. For the sake of clarity, it is not shown on the graph. The current load schedule and possible options for the following load step are presented in the middle graph. The bar chart on the right showcases each model's performance in terms of the corresponding values of root mean square error within the current load step. It outlines the competition between candidates and the change of a trend in dominating deformation mechanism as test goes on. The results of the test indicate that the framework successfully worked as a consolidation sensor. It correctly identified the target model inside the BlackBox along with its material parameters. Table 2 summarises target and best candidate model's outcome. Maximum discrepancy in the parameters values does not exceed 4.5%. This discrepancy was caused by the excessive noise level in the BlackBox output, which often is much smaller in real compaction testing (as shown later in this paper).

It is interesting to examine the resultant load schedule and check whether it displays any characteristic pattern. Typically, these curves are rather complicated, but a few features can be distinguished. For example, on the curve presented in Figure 5, the resulting load schedule demonstrates that the compaction force raises up to 100 N, followed by a dwell stage for 50 seconds. At the last 30 seconds of the test load starts increasing again in a ramp-dwell manner. The resultant load comprises a very wide range of loading rates and a considerable dwell stage at intermediate load. At the early stage of the deformation, the consolidation sensor concludes that the most likely candidates are various forms of incompressible shear flow model along with the correct DefGen candidate. This shows that the initial loading does not provide sufficient data to make a reliable conclusion and a comprehensive test programme for the material characterisation is needed. As indicated in Figure 5 (right side), the process of best model prioritisation runs continuously and is revised at every load step. Hence, the favourable models, defining the load trajectory at the next step, evolve throughout the test. Upon completion of the test, the second-best candidate was defined as a percolation flow model. It was not constant through the test and for the first three load steps sensor defined the second-best candidate as a shear

flow model. As the load schedule became more sophisticated, the accuracy of the shear model decreased significantly, and the percolation model's performance became more robust.

The visualisation of the two-step parameters extraction of one of the candidate models is presented in Figure 6. The process is repeated for every candidate model at each load step through the test. To showcase the initial brute force step, a scatter plot matrix visualising bivariate relationships between the model parameters is depicted in Figure 6.a. It allows revealing the influence of material parameters on the objective function and to gain an insight into possible pitfalls of an optimisation process for a chosen model, such as areas of local minima. There are several areas of local minima visible in Figure 6.a. The actual global minimum and the brute stage result for a given grid density are depicted with red and purple dashed lines correspondingly. As expected, there is a gap between the outcome of the brute optimisation and the target value. It is to be eliminated in the secondary optimisation stage.

Since every consolidation model from the library has three parameters to vary, the optimisation is carried out in four-dimensional space. To illustrate the secondary optimisation process, the residual function is plotted as a three-dimensional grid, where each axis represents one of the material parameters. The value of the residual function is reflected by the size and the colour of a marker. To make the areas of interest more visible, the lower values are depicted with larger marker size and darker colour. This way, local minimum "branches" are clearly seen as illustrated in Figure 6.b. The figure shows how the optimiser avoids getting trapped in the areas of local minimum and converges to the global minimum. As stated in the previous section, the starting point for parameters values is the end result of the initial brute force stage.

To illustrate computational efficiency of the approach, the framework's running time was assessed in concurrent (candidate models are processed simultaneously) and consecutive (candidate models are processed sequentially one after another) operation modes within the proposed virtual exercise. The comparative bar chart reflecting the computational time at each load step is presented in Figure 7. It takes more time to process the first load step as the framework establishes feasible initial set of material parameters for candidate models within the brute force optimisation step. Starting from the second load step there is a gradual increase in processing time for every subsequent step because the compaction data set size expands as the test goes on. Employing the concurrent mode provides a 47% reduction in terms of the overall required computational time comparing to the consecutive mode (280 sec versus 533 sec respectively). Although, these values will vary

for different hardware setups (current setup: CPU Intel Core i7-7700HQ 2.80 GHz, RAM 16 GB 2400 MHz), the predominance of the concurrent data processing approach is clear.

3.5. Validation test

The obtained candidate models were then verified against a different input load schedule. As shown in Figure 5, there is no substantial advantage in terms of the prediction error of the first-best DefGen candidate compared to the second-best percolation one within a single characterisation test. Despite the fact that the target model is predefined and the correct answer is known, the verification stage is still relevant.

Figure 8 illustrated the validation process. A conventional ramp-dwell load programme used in previous studies [12] served as an input for the models. As expected, the best candidate selected by the framework (the DefGen model) adapts to the changed input successfully, whereas the second-best percolation one demonstrates a significant offset in prediction, despite an adequate performance at the characterisation stage. The trials successfully confirmed correct functioning of all sensor's modules. For the considered models, the framework manages to reveal a model type inside the BlackBox along with material parameters after two, sometimes three load steps with high fidelity. One characterisation test always appeared to be sufficient. When testing actual materials, the deformation pattern may be significantly more complicated and show multiple deformation modes. In the event that the proposed framework is not available, a combination of tests with different programmes is required to capture characteristic features of a material's behaviour. It is necessary to minimise the volume of testing programmes without the loss of gain in obtaining information. In this regard, it is interesting to deduce the optimum data-rich testing programmes for the training sets. The next section addresses this problem in application to a material that was extensively characterised in past and for which the DefGen model was found to be efficient.

4. Experimental investigation of data-rich training

4.1. Compaction test set-up

In this section, the importance of a comprehensive test programme for robust material characterisation is demonstrated. A series of experiments with different loading programmes were carried out to explore the compaction behaviour of fibre-reinforced thermosetting prepregs containing thermoplastic tougheners. The prepreg material used was IMA/M21 with a nominal cured ply thickness of 0.184 mm and 59.2% fibre volume fraction [47].

Experimental programmes were designed in a way to incorporate a wide variety of pressure levels, pressure rates in various loading modes - slow monotonic and ramp-dwell regimes. Some programmes were conventional ramp-dwell schedules as used in the literature [12]. Another batch of programmes were inspired by framework's prediction outcomes in a previous section of this paper, where load slowly reaches an intermediate level, dwells, and keeps raising again (Figure 5). The test programmes considered were not aimed to reproduce any particular processing conditions specific to a certain manufacturing method. The end goal was to showcase the advantage of certain loading schedules over the other ones as well as the necessity of multiple experiments to get a data-rich compaction response of the material. Every loading schedule was comprised of five load steps of 240 s each. For a ramp-dwell regime the fastest load application rate was 0.1 MPa/s and was followed by long dwell intervals. In case of a monotonic regime load rate varied between 1.2e-4 and 7.4e-4 MPa/s. An incremental compression force within one load step was specified in a range of 10 N to 30 N. Given the effective loaded area of the tested samples was 15 mm x 15 mm, maximum applied nominal pressure did not exceed 0.5 MPa. Each specimen was tested at a constant temperature of 60℃ throughout the experiment. This temperature was chosen as it is a characteristic temperature at which the transition between flow mechanisms occurs particularly explicitly [28].An insignificantly small compression force of 0.1 N was applied to a specimen prior to the main loading programme in order to establish sufficient contact between the specimen's top surface and the compression platen. Additional dummy tests within the same loading programme but without a specimen were carried out in order to take into account compression rig's compliance. Then, the top platen's displacement as function of time was subtracted from the resulting displacement curve for each sample. The final thickness of the specimen was measured independently immediately after the experiment. To obtain a resulting thickness evolution curve of a specimen, the platen displacement curves were shifted to comply with the resulting thickness value. Such approach eliminates the uncertainty in the initial thickness of a sample. Each test programme was conducted for four samples to ensure repeatability and data consistency. The obtained compaction curves are shown in Figure 9.a.

The experimental testing was carried out using Instron 5969 universal testing machine. A test sample covered in a release film was placed in between custom-built temperature-controlled compression platens as shown in Figure 9.b. A control thermocouple and a thick film conduction heater were attached to each platen to ensure that specified temperature conditions are met. The testing apparatus allows to transfer controlled load to the

specimen within an isothermal programme and to measure corresponding compaction response of the material. It was necessary to ensure steady contact between neighbouring plies during compression. Material tends to spread transversely as the plies are squeezed from underneath the area under compression. For that reason, following [12] test specimens were laid up in a cruciform configuration to allow plies to remain in contact as shown in Figure 9.c. The baseline area under compression is 15 mm x 15 mm.

The test specimens were manufactured in a clean room following standard lay-up guidelines. All specimens were laid-up in a 16 plies cross-ply (CP) configuration $[90/0]_8$ with a total thickness of ~3.2 mm. During lay-up at room temperature ten-minute debulking routine was carried out for every four plies. Upon manufacturing, specimens' dimensions were measured by digital Vernier callipers.

4.2. Results processing and discussion

To identify the data-rich testing programme from which the maximum information can be collected whilst performing the smallest amount of experiments, compaction results from different loading programmes were arbitrarily split into separate validation and training sets. The size of the training set was capped to a maximum of three tests. In this example tests 1, 4 and 8 formed a pool of tests for model characterisation. The remaining tests were left for model validation. At the stage of model definition all possible combinations of loading schedules from a group of characterisation tests defined input training sets as shown in Table 3. The size of the set was ranging from just one test to a maximum size of three. A separate analysis for every training set was carried out, meaning that a parameters extraction routine for each model from the consolidation library was performed to fit joint compaction curves from a training set.

After the characterisation stage, the developed models had to be trialled against a different input of compaction data. The models were put to the test against each batch of data in the validation set and the cumulative error in prediction served as a model's performance measure. Given the total number of tests conducted and the maximum training set size, the size of the validation set was fixed at the size of five programmes. An overview of training and validation sets structure is presented in Table 3.

The parameters extraction procedure results for the training set comprised of tests (1, 4, 8) are presented below. Figure 10 presents a ranking bar chart for all seven possible training sets. Several conclusions can be made upon examination of the results. The general trend of experimental outcomes follows the theoretical predictions with regard to the importance of data-rich compaction response of the material. The findings

confirm that the input sets comprised of more diverse loading programmes demonstrate a superior performance on a validation data set.

Because of the sheer volume of obtained data, only two characteristic examples are shown in this paper. Models trained on fully populated data-rich training set (1, 4, 8) (Figure 11.a) are more capable of predicting material compaction response within the validation loading schedules as illustrated in Figure 11.c. On the contrary, models based on the training set (8,) demonstrate a significant drop in accuracy as shown in Figure 11.d. As expected, formulated models showcase an impeccable efficiency in fitting just one input set from test 8 at the training stage Figure 11.b. However, there is a substantial offset between experimental compaction curves and model's output at the validation phase (Figure 11.d). It results in a 30.0 % error raise compared to the baseline value. It is a clear indication of an insufficient input training data. Candidate models were not exposed to a variety of loading schedules at the formulation phase and did not capture the material's response to changing processing conditions. Consequently, they are worse at predicting thickness evolution for experimental programmes with different load amplitudes and load application rates. The resulting candidate models and parameters within both training sets are presented in Table 4.

The results shown in Figure 10 indicate that there is no substantial advantage of the full training set over the second-best training combination (4, 8). The difference in total error in thickness prediction between these input options is 0.1%. That is to say, conducting characterisation test 1 does not bring a considerable value to the training set (4, 8) and can be omitted. The same accuracy can be obtained with a smaller number of tests. Additionally, there is an outlying phenomenon which stands out from the observed trend. The fourth-best training set (1,) is advantageous in comparison to (1, 4). It means that adding test 4 to an input training set (1,) impairs the final result. The most likely explanation of such phenomenon is that the validation set is underpopulated. It is important to note that every candidate model from the library has its own limitations and might not be able to reflect the material behaviour for a certain load set within specified processing conditions. A more diverse validation set would require conducting more characterisation tests. From the outcome of these experiments, it is possible to conclude that the current number of tests for validation is sufficient.

5. Conclusion

Upon review of the experimental results presented in this paper, the question arises as to how to build an appropriate /rational /data-rich testing programme. It is fundamentally important for modelling composite manufacturing processes. It was clearly illustrated that deficient and insufficient testing may lead to fundamentally wrong predictions of material states and completely mislead the results of process optimisation procedure. In many cases the underlying physical mechanisms are difficult to know in advance and wrong subjective assumption about the flow modes will lead to conceptual mistake in understanding materials' behaviour. In the current environment when materials become multi-functional and contain a lot of additives to enhance their performances, it becomes increasingly difficult to know the right flow mode in advance. Moreover, as has been established previously [12,26,28], the same material may exhibit different deformation responses when temperature varies within a relatively small range.

The new "consolidation sensor" framework, presented here, has the potential to address these challenges and to remove the subjective judgement about the material behaviour. The framework was initially challenged in a virtual test and limited by few known material models. However, it is clear that this framework can be reinforced further by enriching the material library. The computational efficiency of the framework also appears to be quite promising and suitable for testing in a real environment. The approach presented here shows the potential to be implemented in real-time, in a reactive manner. The experiment's outcomes showcased candidate models' evolution in a step-by-step process and proved the consolidation sensor's capability to investigate material models. The identification of the pure flow modes may also be useful to decode dominant mechanisms at different stages of deformation such as fibre shear, resin bleeding or a transition from one mode to another. Current tests were performed at a constant temperature. The obtained models are not guaranteed to perform on the same level within different processing conditions. Taking temperature effects into account would lead to an introduction of temperature-dependant material parameters. Consequently, it would make the characterisation and properties extraction task more challenging due to the increased parameters space. In the current study the proposed framework has proven its efficiency in handling complex models and developing data-rich testing programmes.

The proposed adaptive testing approach has potential for application to various problems beyond the scope of the consolidation study for composite precursors presented here. Potentially, it could be relevant for any multi-component compliant material (soils, powders, food etc) which exhibit complex behaviour under

processing or service conditions. Applying this methodology to a different multi-material system would require populating the library with the new candidate models that can adequately reflect the response of the studied system. It is also envisaged that this methodology could be applied well beyond the scope of the compaction testing. Similar challenges in characterisation of materials can be seen in various other testing campaigns. This includes, for instance, testing of precursors that is required for simulation of AFP deposition/forming/liquid moulding, such as identifying suitable models for the behaviour of prepregs/preforms in in-plane or inter-ply shear, friction, and tack. The critical factor for successful identification of deformation modes is to include physical models representative of those that may take place.

Acknowledgements:

This work was supported by the Engineering and Physical Sciences Research Council (EPSRC) through the Centre for Doctoral Training in Advanced Composites Collaboration for Innovation and Science (grant number EP/L016028/1) and SIMulation of new manufacturing PROcesses for Composite Structures (SIMPROCS) (grant number EP/P027350/1).

References:

[1] Belnoue JPH, Hallett SR. A rapid multi-scale design tool for the prediction of wrinkle defect formation in composite components. Mater Des 2020;187. https://doi.org/10.1016/j.matdes.2019.108388.

[2] Matveev MY, Belnoue JPH, Nixon-Pearson OJ, Ivanov DS, Long AC, Hallett SR, et al. A numerical study of variability in the manufacturing process of thick composite parts. Compos Struct 2019;208:23–32. https://doi.org/10.1016/j.compstruct.2018.09.092.

[3] Hubert P, Poursartip A. Aspects of the Compaction of Composite Angle Laminates: An Experimental Investigation. J Compos Mater 2001;35:2–26. https://doi.org/10.1177/002199801772661849.

[4] Hubert P, Vaziri R, Poursartip A. A two-dimensional flow model for the process simulation of complex shape composite laminates. Int J Numer Methods Eng 1999;44:1–26. https://doi.org/10.1002/(SICI)1097-0207(19990110)44:1<1::AID-NME481>3.0.CO;2-K.

[5] Paterson DT, Eaves TS, Hewitt DR, Balmforth NJ, Martinez DM. Flow-driven compaction of a fibrous porous medium. Phys Rev Fluids 2019;4:1–28. https://doi.org/10.1103/PhysRevFluids.4.074306.

[6] Haghdan S, Tannert T, Smith GD. Effects of reinforcement configuration and densification on impact strength of wood veneer/polyester composites. J Compos Mater 2015;49:1161–70. https://doi.org/10.1177/0021998314531308.

[7] Castellanos D, Martin PJ, Butterfield J, McCourt M, Kearns M, Cassidy P. Sintering and densification of fibre reinforcement in polymers during rotational moulding. Procedia Manuf 2020;47:980–6. https://doi.org/10.1016/j.promfg.2020.04.301.

[8] Lightfoot JS, Wisnom MR, Potter K. A new mechanism for the formation of ply wrinkles due to shear between plies. Compos Part A Appl Sci Manuf 2013;49:139–47. https://doi.org/10.1016/j.compositesa.2013.03.002.

[9] Phillips R, Akyüz DA, Månson JAE. Prediction of the consolidation of woven fibre-reinforced thermoplastic composites. Part I. Isothermal case. Compos Part A Appl Sci Manuf 1998;29:395–402. https://doi.org/10.1016/S1359-835X(97)00099-7.

[10] Wang EL, Gutowski TG. Laps and gaps in thermoplastic composites processing. Compos Manuf 1991;2:69–78. https://doi.org/https://doi.org/10.1016/0956-7143(91)90182-G.

[11] Ivanov DS, Lomov S V. Modeling of 2D and 3D woven composites. In: Irving; P, Soutis C, editors.

Polym. Compos. Aerosp. Ind. (Second Ed., Woodhead Publishing; 2019, p. 23–57. https://doi.org/10.1016/B978-0-08-102679-3.00002-2.
[12] Nixon-Pearson OJ, Belnoue JPH, Ivanov DS, Potter KD, Hallett SR. An experimental investigation of the consolidation behaviour of uncured prepregs under processing conditions. J Compos Mater 2017;51:1911–24. https://doi.org/10.1177/0021998316665681.
[13] Barnes JA, Cogswell FN. Transverse flow processes in continuous fibre-reinforced thermoplastic composites. Composites 1989;20:38–42. https://doi.org/10.1016/0010-4361(89)90680-0.
[14] Salvatori D, Caglar B, Teixidó H, Michaud V. Permeability and capillary effects in a channel-wise non-crimp fabric. Compos Part A Appl Sci Manuf 2018;108:41–52. https://doi.org/10.1016/j.compositesa.2018.02.015.
[15] Li X, Hallett SR, Wisnom MR. Modelling the effect of gaps and overlaps in automated fibre placement (AFP)-manufactured laminates. Sci Eng Compos Mater 2015;22:115–29. https://doi.org/10.1515/secm-2013-0322.
[16] Gu Y, Xin C, Li M, Cheng Y, Zhang Z. Resin pressure and resin flow inside tapered laminates during zero-bleeding and bleeding processes. J Reinf Plast Compos 2012;31:205–14. https://doi.org/10.1177/0731684411434149.
[17] Hubert P, Johnston A, Poursartip A, Nelson K. Cure kinetics and viscosity models for Hexcel 8552 epoxy resin. Int SAMPE Symp Exhib 2001;46 II:2341–54.
[18] Zhu J, Wei S, Yadav A, Guo Z. Rheological behaviors and electrical conductivity of epoxy resin nanocomposites suspended with in-situ stabilized carbon nanofibers. Polymer (Guildf) 2010;51:2643–51. https://doi.org/10.1016/j.polymer.2010.04.019.
[19] Ghnatios C, Chinesta F, Binetruy C. 3D Modeling of squeeze flows occurring in composite laminates. Int J Mater Form 2015;8:73–83. https://doi.org/10.1007/s12289-013-1149-4.
[20] Kelly PA. A viscoelastic model for the compaction of fibrous materials. J Text Inst 2011;102:689–99. https://doi.org/10.1080/00405000.2010.515103.
[21] Meeten GH. Yield stress of structured fluids measured by squeeze flow. Rheol Acta 2000;39:399–408. https://doi.org/10.1007/s003970000071.
[22] Campanella OH, Peleg M. Squeezing flow viscometry for nonelastic semiliquid foods - Theory and applications. Crit Rev Food Sci Nutr 2002;42:241–64. https://doi.org/10.1080/10408690290825547.
[23] Hubert P, Poursartip A. A method for the direct measurement of the fibre bed compaction curve of composite prepregs. Compos Part A Appl Sci Manuf 2001;32:179–87. https://doi.org/10.1016/S1359-835X(00)00143-3.
[24] Belnoue J, Ivanov D, Hallett SR, Nixon-Pearson OJ, P-H Belnoue J, Ivanov DS. The compaction behaviour of un-cured prepregs. 20th Int Conf Compos Mater 2015.
[25] Lukaszewicz DHJA, Potter K. Through-thickness compression response of uncured prepreg during manufacture by automated layup. Proc Inst Mech Eng Part B J Eng Manuf 2012;226:193–202. https://doi.org/10.1177/0954405411411817.
[26] Belnoue JPH, Nixon-Pearson OJ, Ivanov D, Hallett SR. A novel hyper-viscoelastic model for consolidation of toughened prepregs under processing conditions. Mech Mater 2016;97:118–34. https://doi.org/10.1016/j.mechmat.2016.02.019.
[27] Mario A. Valverde, Belnoue JP-H, Kupfer R, Kawashita LF, Gude M, Hallett SR. Compaction behaviour of continuous fibre-reinforced thermoplastic composites under rapid processing conditions. Compos Part A 2021.
[28] Ivanov Dmitry, Yiqing Li , Ward Carwyn PK. Transitional behaviour of prepregs in automated fibre deposition processes. Proc 19th Int Conf Compos Mater 2013.
[29] Belnoue JPH, Nixon-Pearson OJ, Thompson AJ, Ivanov DS, Potter KD, Hallett SR. Consolidation-driven defect generation in thick composite parts. J Manuf Sci Eng Trans ASME 2018;140. https://doi.org/10.1115/1.4039555.
[30] Belnoue JPH, Mesogitis T, Nixon-Pearson OJ, Kratz J, Ivanov DS, Partridge IK, et al. Understanding and predicting defect formation in automated fibre placement pre-preg laminates. Compos Part A Appl Sci Manuf 2017;102:196–206. https://doi.org/10.1016/j.compositesa.2017.08.008.
[31] Martin J, Adana DDR de, Asuero AG. Fitting Models to Data: Residual Analysis, a Primer. In: Hessling JP, editor. Uncertain. Quantif. Model Calibration, InTech; 2017. https://doi.org/10.5772/68049.
[32] Laxalde J, Ruckebusch C, Devos O, Caillol N, Wahl F, Duponchel L. Characterisation of heavy oils using near-infrared spectroscopy: Optimisation of pre-processing methods and variable selection.

Anal Chim Acta 2011;705:227–34. https://doi.org/10.1016/j.aca.2011.05.048.
[33] Vijayaraghavan V, Garg A, Lam JSL, Panda B, Mahapatra SS. Process characterisation of 3D-printed FDM components using improved evolutionary computational approach. Int J Adv Manuf Technol 2015;78:781–93. https://doi.org/10.1007/s00170-014-6679-5.
[34] Sandberg M, Kabachi A, Volk M, Bo Salling F, Ermanni P, Hattel JH, et al. Permeability and compaction behaviour of air-texturised glass fibre rovings: A characterisation study. J Compos Mater 2020;54:4241–52. https://doi.org/10.1177/0021998320926703.
[35] Chan KY, Kwong CK, Dillon TS, Tsim YC. Reducing overfitting in manufacturing process modeling using a backward elimination based genetic programming. Appl. Soft Comput. J., vol. 11, 2011, p. 1648–56. https://doi.org/10.1016/j.asoc.2010.04.022.
[36] Jouan-Rimbaud D, Massart DL, De Noord OE. Random correlation in variable selection for multivariate calibration with a genetic algorithm. Chemom Intell Lab Syst 1996;35:213–20. https://doi.org/10.1016/S0169-7439(96)00062-7.
[37] Vanhuyse J, Deckers E, Jonckheere S, Pluymers B, Desmet W. Global optimisation methods for poroelastic material characterisation using a clamped sample in a Kundt tube setup. Mech Syst Signal Process 2016;68–69:462–78. https://doi.org/10.1016/j.ymssp.2015.06.027.
[38] Green JEF, Friedman A. The extensional flow of a thin sheet of incompressible, transversely isotropic fluid. Eur J Appl Math 2008;19:225–57. https://doi.org/10.1017/S0956792508007377.
[39] Brocks W, Scheider I, Steglich D. Hybrid Methods for Material Characterisation. Int J Pure Appl Math 2008;49:553–8.
[40] Van Rossum G, Python Dev Team. Python 3.6 Language Reference. Samurai Media Limited; 2016.
[41] Newville M, Stensitzki T, Allen DB, Ingargiola A. LMFIT: Non-Linear Least-Square Minimization and Curve-Fitting for Python. 2018. https://doi.org/10.5281/zenodo.11813.
[42] Gao F, Han L. Implementing the Nelder-Mead simplex algorithm with adaptive parameters. Comput Optim Appl 2012;51:259–77. https://doi.org/10.1007/s10589-010-9329-3.
[43] Rao CR, Toutenburg H. Linear Models: Least Squares and Alternatives, Second Edition. Springer; 1999.
[44] Wales DJ, Doye JPK. Global Optimization by Basin-Hopping and the Lowest Energy Structures of Lennard-Jones Clusters Containing up to 110 Atoms. J Phys Chem A 1997;101:5111–5116. https://doi.org/10.1021/jp970984n.
[45] Storn R, Price K. Differential Evolution-A Simple and Efficient Heuristic for Global Optimization over Continuous Spaces. J Glob Optim 1997;11:341–59. https://doi.org/10.1023/A:1008202821328.
[46] Ramalho L. Fluent Python: Clear, concise, and effective programming. O'Reilly Media, Inc.; 2015.
[47] HexPly ® M21 180°C (350°F) curing epoxy matrix. Epoxy Matrix Product Datasheet. 2015.
[48] Rogers TG. Squeezing flow of fibre-reinforced viscous fluids. J Eng Math 1989;23:81–9. https://doi.org/10.1007/BF00058434.
[49] Pipes RB. Anisotropic Viscosities of an Oriented Fiber Composite with a Power-Law Matrix. J Compos Mater 1992;26:1536–52. https://doi.org/10.1177/002199839202601009.
[50] Shahsavari S, McKinley GH. Mobility of power-law and Carreau fluids through fibrous media. Phys Rev E - Stat Nonlinear, Soft Matter Phys 2015;92. https://doi.org/10.1103/PhysRevE.92.063012.
[51] Servais C, Luciani A, Månson J-AE. Squeeze flow of concentrated long fibre suspensions: experiments and model. J Nonnewton Fluid Mech 2002;104:165–84. https://doi.org/10.1016/S0377-0257(02)00018-6.
[52] Gutowski TG, Cai Z, Bauer S, Boucher D, Kingery J, Wineman S. Consolidation Experiments for Laminate Composites. J Compos Mater 1987;21:650–69. https://doi.org/10.1177/002199838702100705.
[53] Gutowski TG, Morigaki T, Cai Z. The Consolidation of Laminate Composites. J Compos Mater 1987;21:172–88. https://doi.org/10.1177/002199838702100207.
[54] Gutowski TG, Dillon G. The Elastic Deformation of Lubricated Carbon Fiber Bundles: Comparison of Theory and Experiments. J Compos Mater 1992;26:2330–47. https://doi.org/10.1177/002199839202601601.
[55] Gebart BR. Permeability of Unidirectional Reinforcements for RTM. J Compos Mater 1992;26:1100–33. https://doi.org/10.1177/002199839202600802.

Figure 1: a, b – training/validation test programs, c,d – the first example of model's overfit, where RMSE is root mean square error., e,f – the second example of local minimum encounter.

Figure 2: a – possible load schedule options in a real-time testing, b – detailed algorithm of the consolidation sensor

Figure 3: Optimisation routine flow chart

Figure 4: BlackBox module's algorithm.

Figure 5: Virtual testing step by step routine.

Figure 6: Parameters extraction visualization. a – initial stage brute force optimisation heatmap. b – secondary stage optimisation path within an objective function's mesh grid.

Figure 7: Consolidation framework's promptness within each step of the test in consecutive and concurrent processing modes.

Figure 8: Candidate models validation

Figure 9: a – conducted load programmes and corresponding compaction response, b – temperature-controlled compression platens, test specimen in a release film, c –test specimen.

Figure 10: Training sets ranking

Figure 11: a – two best performing candidate models fit experimental data for (1, 4, 8) training set, b – two best performing candidate models fit experimental data for (8) training set, c – validation of two best performing candidate models based on (1, 4, 8) training set, d – validation of two best performing candidate models based on (8) training set

Table 1: Summary of selected flow models for unidirectional fibre-resin suspensions

Flow mode type	F(t, h)	Q(h)	Material parameters
Incompressible shear flow of Newtonian suspension in the transverse direction [48]			
Zero friction with tool and constant tool-material contact (nfcc)	$P_{applied}$	$\frac{h}{4\,\eta}$	η
Zero friction with tool and evolving tool-material contact (nfvc)	$P_{applied}$	$\frac{h^2}{4\,\eta h_0}$	η
No-slip conditions and constant tool-material contact (nscc)	$P_{applied}$	$\frac{h^4}{\eta h_0 (w^2 + 3h^2)}$	η
No-slip conditions, evolving tool-material contact (nsvc)	$P_{applied}$	$\frac{h^6}{\eta h_0 (w_0^2 h_0^2 + 3h^4)}$	η
Incompressible shear flow in the transverse direction with power law shear thinning [49–51]			
Zero friction with tool and constant tool-material contact (nfcc_pow)	$\sqrt[n]{P_{applied}}$	$\sqrt[n]{\frac{1}{4\eta_0\,\lambda^{n-1}}}h$	η_0 λ n
Zero friction with tool and evolving tool-material contact (nfvc_pow)	$\sqrt[n]{P_{applied}}$	$\sqrt[n]{\frac{1}{4\,\eta_0\lambda^{n-1}\ h_0}}h^{\frac{n+1}{n}}$	η_0 λ n
No-slip conditions and constant tool-material contact (nscc_pow)	$\sqrt[n]{P_{applied}}$	$\sqrt[n]{\frac{1}{\lambda^{n-1}\,\eta_0 h_0 (w^2 + 3h^2)}}h^{\frac{n+3}{n}}$	η_0 λ n

No-slip conditions, evolving tool-material contact (nsvc_pow)	$\sqrt[n]{P_{applied}}$	$\sqrt[n]{\frac{1}{\lambda^{n-1}\,\eta_0 h_0 (w_0^2 h_0^2 + 3h^4)}}\, h^{\frac{n+5}{n}}$	η_0 λ n
Percolation flow of compressible tape under additive superposition of resin pressure and fibre bed response [52–54]			
Flow in the longitudinal direction (bgc)	$P_{applied}$ $- P_{pre}(h)$	$\frac{3K(h)}{\tilde{\eta} {w_0}^2} h$	$\tilde{\eta}$ K_A σ_A
Empirical model for transition behaviour of toughened prepreg with features of shear and percolation flows [26]			
DefGen model (defgen)	$\sqrt[a+1]{P_{applied}}$	$-\sqrt[a+1]{\frac{1}{\overline{\eta_{micro}} \cdot \eta_{ply} \cdot \overline{\eta_{rate}}}} \cdot h$	a b k

where h_0 – initial thickness, t - time, $P_{applied}$ – pressure applied to the top surface of a composite precursor, η – viscosity of incompressible Newtonian suspension, η_0 – zero-shear-rate viscosity, $\tilde{\eta}$ – the viscosity of resin, f- current fibre volume fraction, $K(f) = K_A \frac{(1-f)^3}{f^2}$ – permeability function [55], $P_{pre}(h) = \sigma_A \frac{\sqrt{f/f_0}-1}{(\sqrt{f_{lim}/f}-1)^4}$ – fibre bed response, where σ_A is the material spring constant, f_0 is the initial fibre volume fraction, f_{lim} is the maximum achievable fibre volume fraction, w_0 – width of a specimen, n – power-law exponent, a,b,k – DefGen material parameters [26]

Table 2: Virtual experimentation outcomes

	Model type	Parameter 1	Parameter 2	Parameter 3
Target model inside Blackbox	DefGen	a: -0.8378	b: -12.96	k: 0.7953
Candidate model 1	DefGen	a: -0.8015	b: -12.81	k: 0.7991
Candidate model 2	Percolation (bgc)	$K_A/\tilde{\eta}$: 0.9143	σ_A: 0.0080	

Table 3 - Training and verification sets. Numbers in parentheses represent test numbers.

Training set	Validation set
(1,)	(2, 3, 5, 6, 7)
(4,)	(2, 3, 5, 6, 7)
(8,)	(2, 3, 5, 6, 7)
(1, 4)	(2, 3, 5, 6, 7)
(1, 8)	(2, 3, 5, 6, 7)
(4, 8)	(2, 3, 5, 6, 7)
(1, 4, 8)	(2, 3, 5, 6, 7)

Table 4: Candidate models within different training sets.

	Model type	Parameter 1	Parameter 2	Parameter 3
		Training set (1, 4, 8)		
Candidate model 1	DefGen	a: -0.8616	b: -14.41	k: 0.8324
Candidate model 2	Percolation (bgc)	$K_A/\tilde{\eta}$: 0.4567	σ_A: 0.0052	
		Training set (8,)		
Candidate model 1	DefGen	a: -0.5000	b: -12.35	k: 0.8533
Candidate model 2	Percolation (bgc)	$K_A/\tilde{\eta}$: 0.4785	σ_A: 0.0039	

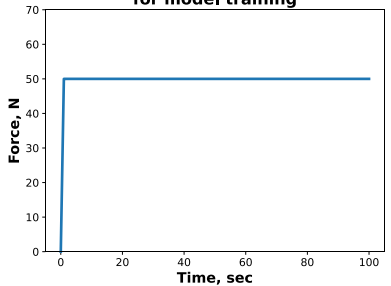
Load schedule
for model training
Force, N
Time, sec

a)

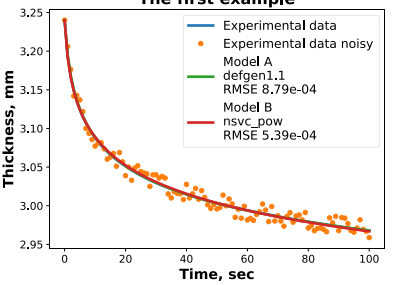
Training response
The first example
Thickness, mm
Time, sec
Experimental data
Experimental data noisy
Model A
defgen1.1
RMSE 8.79e-04
Model B
nsvc_pow
RMSE 5.39e-04

c)

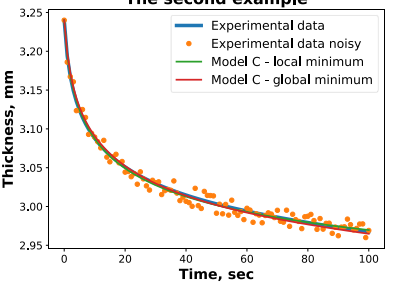
Training response
The second example
Thickness, mm
Time, sec
Experimental data
Experimental data noisy
Model C - local minimum
Model C - global minimum

e)

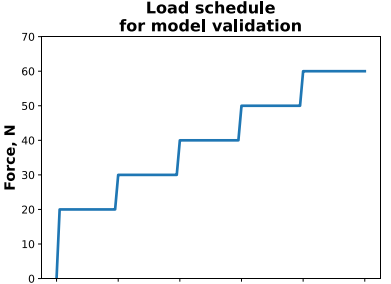
Load schedule
for model validation
Force, N
Time, sec

b)

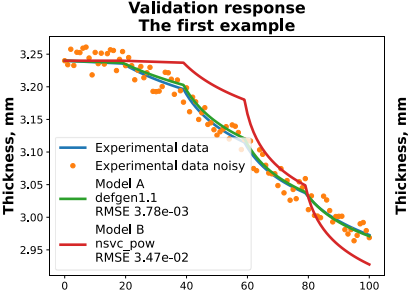
Validation response
The first example
Thickness, mm
Time, sec
Experimental data
Experimental data noisy
Model A
defgen1.1
RMSE 3.78e-03
Model B
nsvc_pow
RMSE 3.47e-02

d)

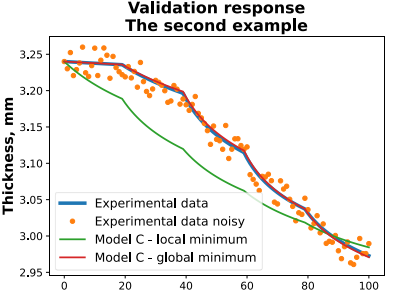
Validation response
The second example
Thickness, mm
Time, sec
Experimental data
Experimental data noisy
Model C - local minimum
Model C - global minimum

f)

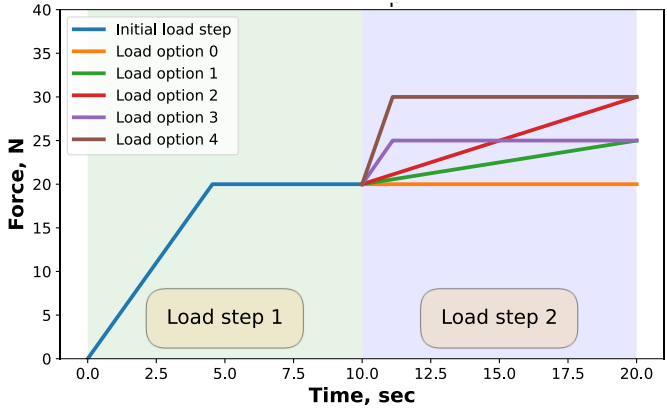
Initial load step
Load option 0
Load option 1
Load option 2
Load option 3
Load option 4
Force, N
Time, sec
Load step 1
Load step 2

a)

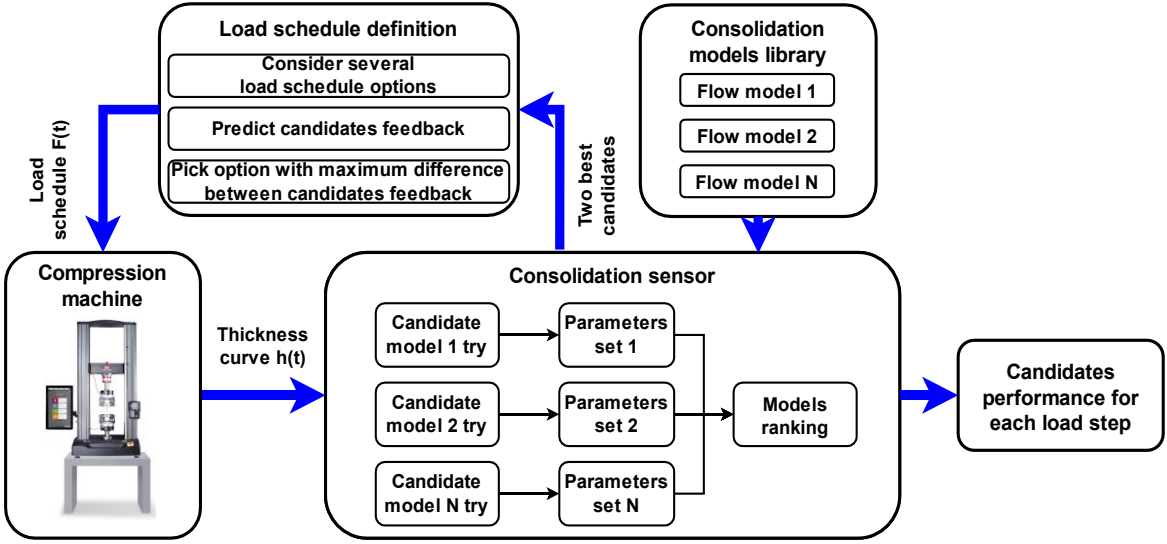
Load schedule definition
Consider several load schedule options
Predict candidates feedback
Pick option with maximum difference between candidates feedback
Consolidation models library
Flow model 1
Flow model 2
Flow model N
Load schedule F(t)
Two best candidates
Compression machine
Thickness curve h(t)
Consolidation sensor
Candidate model 1 try
Candidate model 2 try
Candidate model N try
Parameters set 1
Parameters set 2
Parameters set N
Models ranking
Candidates performance for each load step

b)

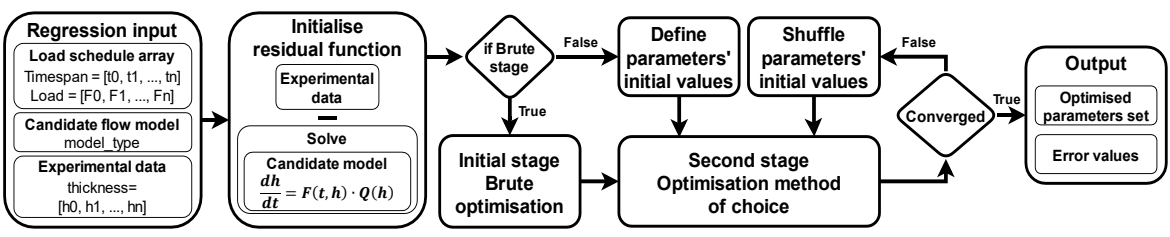
Regression input
Load schedule array
Timespan = [t0, t1, ..., tn]
Load = [F0, F1, ..., Fn]
Candidate flow model
model_type
Experimental data
thickness=
[h0, h1, ..., hn]
Initialise residual function
Experimental data
−
Solve
Candidate model
$\frac{dh}{dt} = F(t,h) \cdot Q(h)$
if Brute stage
False
True
Define parameters' initial values
Shuffle parameters' initial values
False
Converged
True
Output
Optimised parameters set
Error values
Initial stage Brute optimisation
Second stage Optimisation method of choice

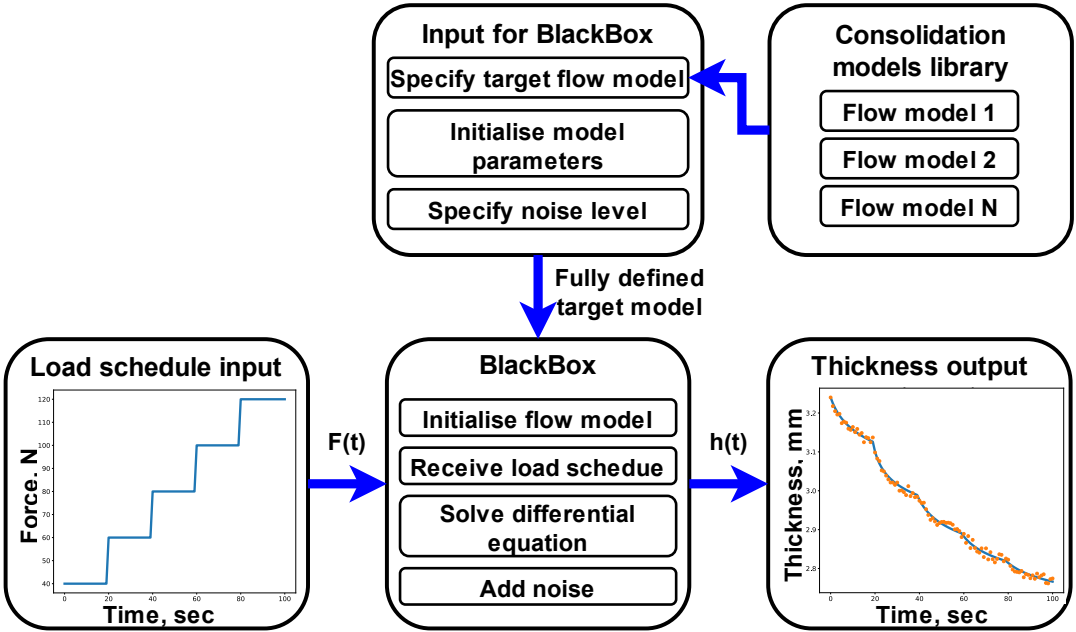
Input for BlackBox
Specify target flow model
Initialise model parameters
Specify noise level
Consolidation models library
Flow model 1
Flow model 2
Flow model N
Fully defined target model
Load schedule input
Force. N
Time, sec
F(t)
BlackBox
Initialise flow model
Receive load schedue
Solve differential equation
Add noise
h(t)
Thickness output
Thickness, mm
Time, sec

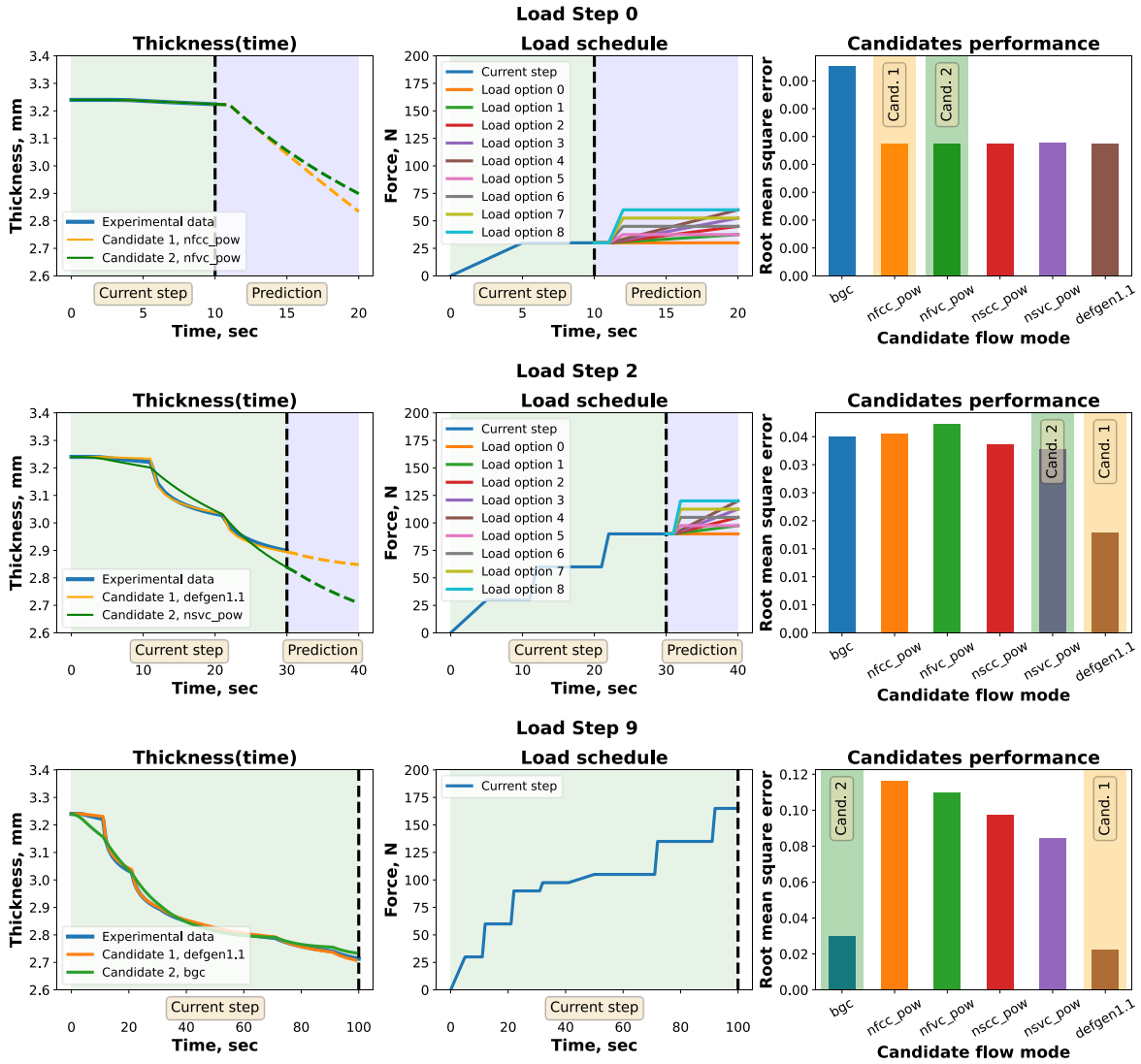
Load Step 0
Thickness(time)
Thickness, mm
Time, sec
Experimental data
Candidate 1, nfcc_pow
Candidate 2, nfvc_pow
Current step
Prediction
Load schedule
Force, N
Load option 0
Load option 1
Load option 2
Load option 3
Load option 4
Load option 5
Load option 6
Load option 7
Load option 8
Candidates performance
Root mean square error
Cand. 1
Cand. 2
bgc
nfcc_pow
nfvc_pow
nscc_pow
nsvc_pow
defgen1.1
Candidate flow mode
Load Step 2
Thickness(time)
Experimental data
Candidate 1, defgen1.1
Candidate 2, nsvc_pow
Load schedule
Candidates performance
Load Step 9
Thickness(time)
Experimental data
Candidate 1, defgen1.1
Candidate 2, bgc
Load schedule
Candidates performance

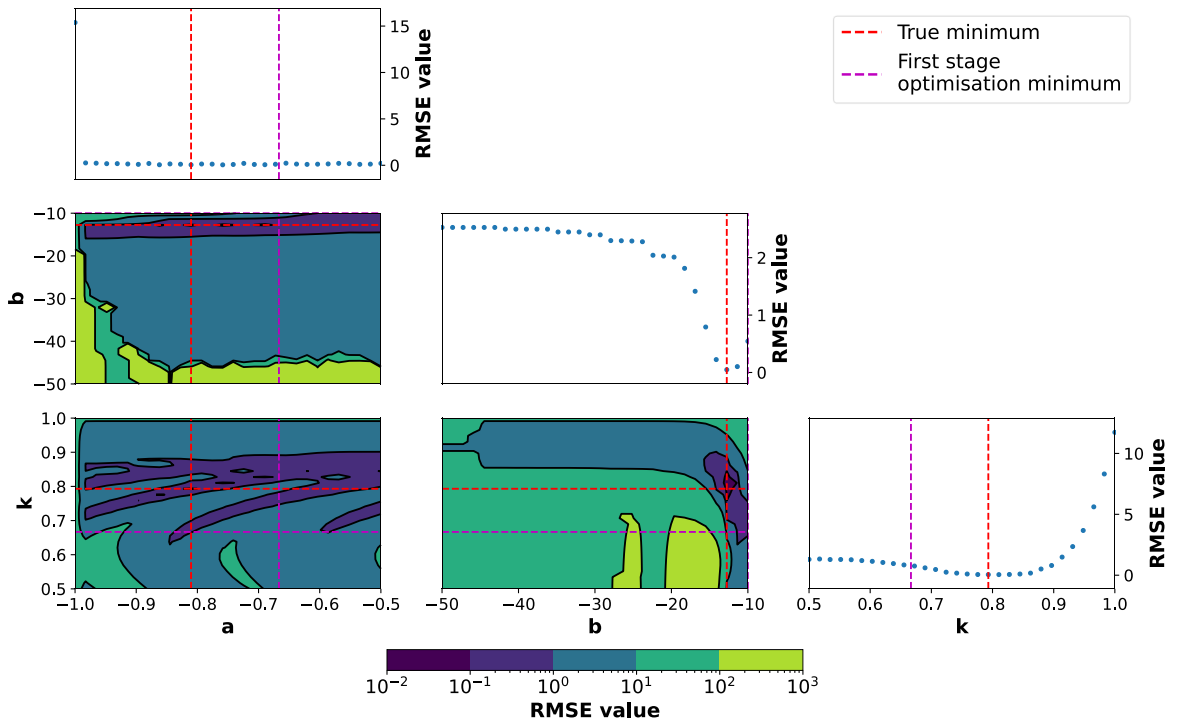
True minimum
First stage optimisation minimum
RMSE value
a
b
k
RMSE value

a)

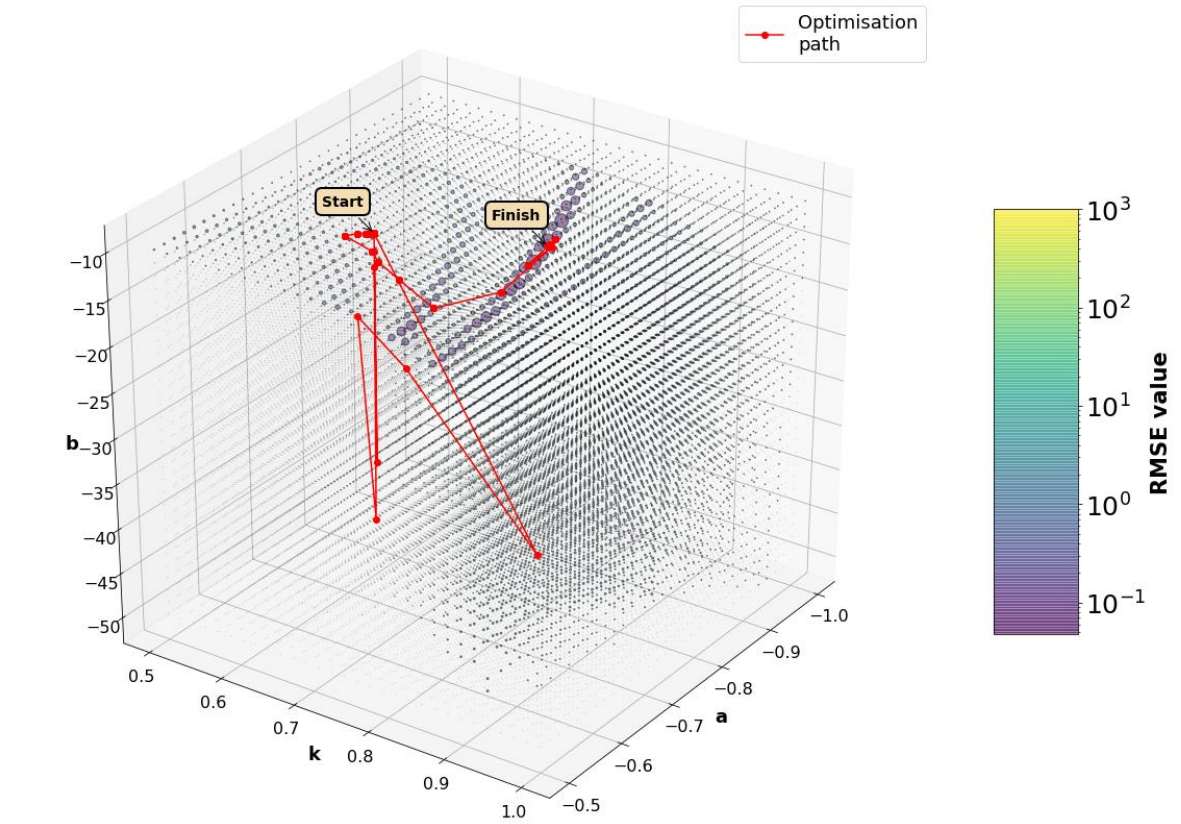
Optimisation path
Start
Finish
b
k
a
RMSE value

b)

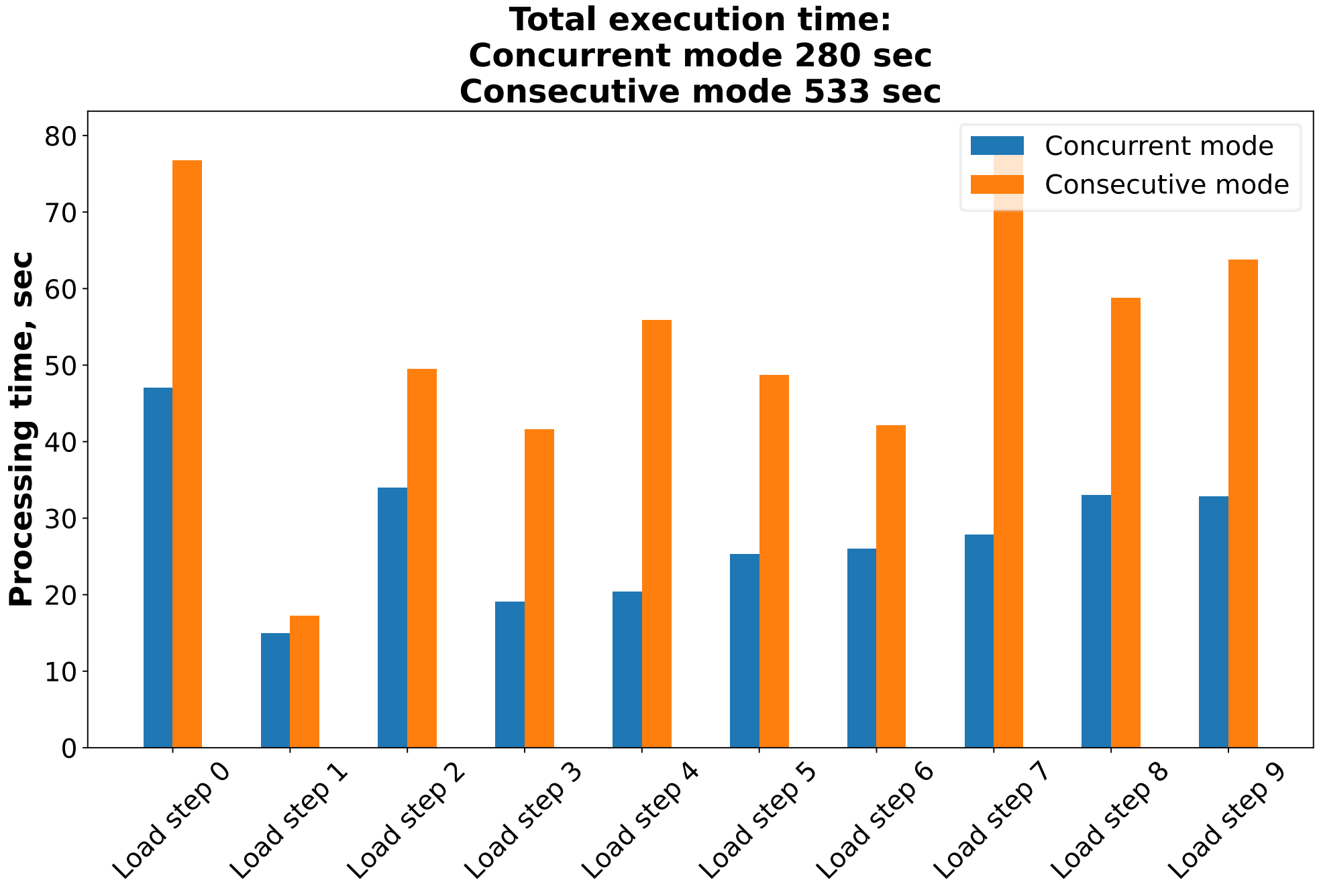
Total execution time:
Concurrent mode 280 sec
Consecutive mode 533 sec
Processing time, sec
0
10
20
30
40
50
60
70
80
Concurrent mode
Consecutive mode
Load step 0
Load step 1
Load step 2
Load step 3
Load step 4
Load step 5
Load step 6
Load step 7
Load step 8
Load step 9

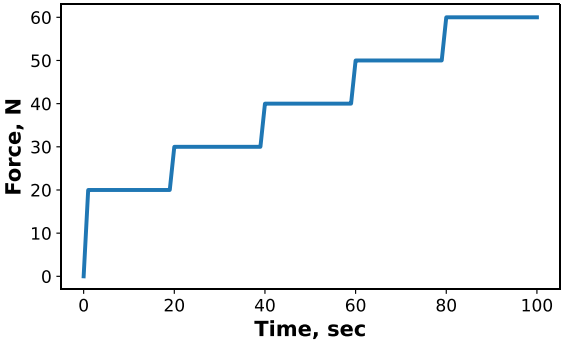
Load schedule for model validation
Force, N
Time, sec
0
10
20
30
40
50
60
0
20
40
60
80
100

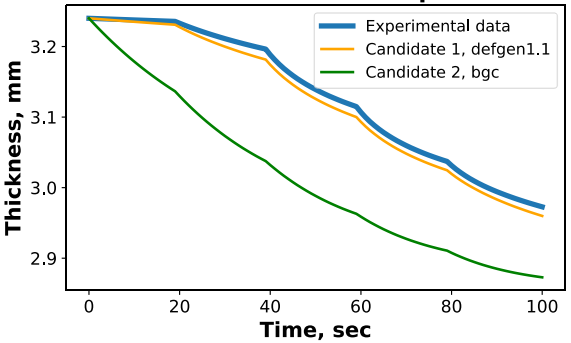
Models validation response
Thickness, mm
Time, sec
Experimental data
Candidate 1, defgen1.1
Candidate 2, bgc
2.9
3.0
3.1
3.2
0
20
40
60
80
100

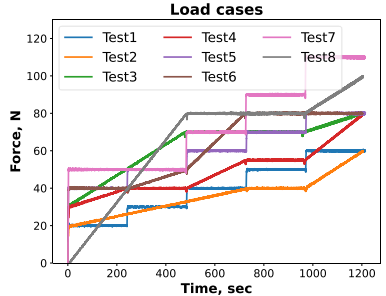
Load cases
Test1
Test2
Test3
Test4
Test5
Test6
Test7
Test8
Force, N
Time, sec
0
20
40
60
80
100
120
0
200
400
600
800
1000
1200

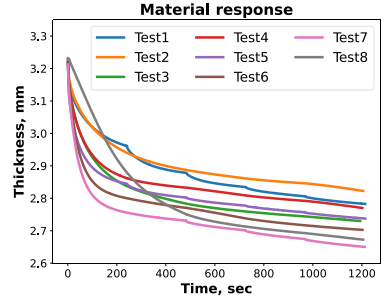
Material response
Test1
Test2
Test3
Test4
Test5
Test6
Test7
Test8
Thickness, mm
Time, sec
2.6
2.7
2.8
2.9
3.0
3.1
3.2
3.3
0
200
400
600
800
1000
1200

a)

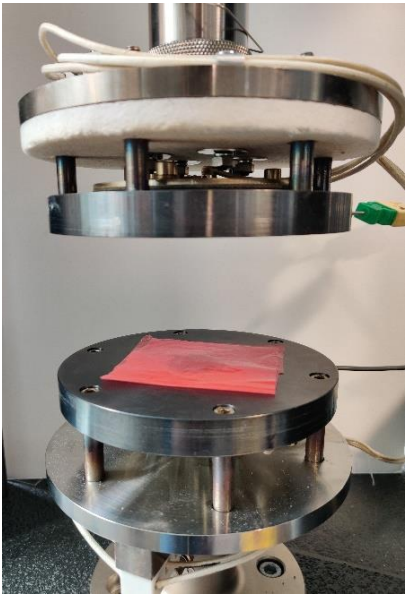

b)

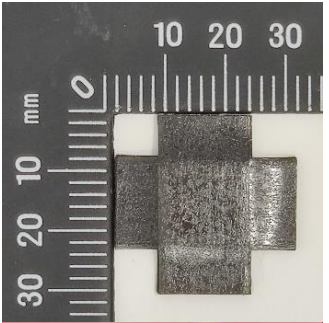
10
20
30
0
mm
10
20
30

c)

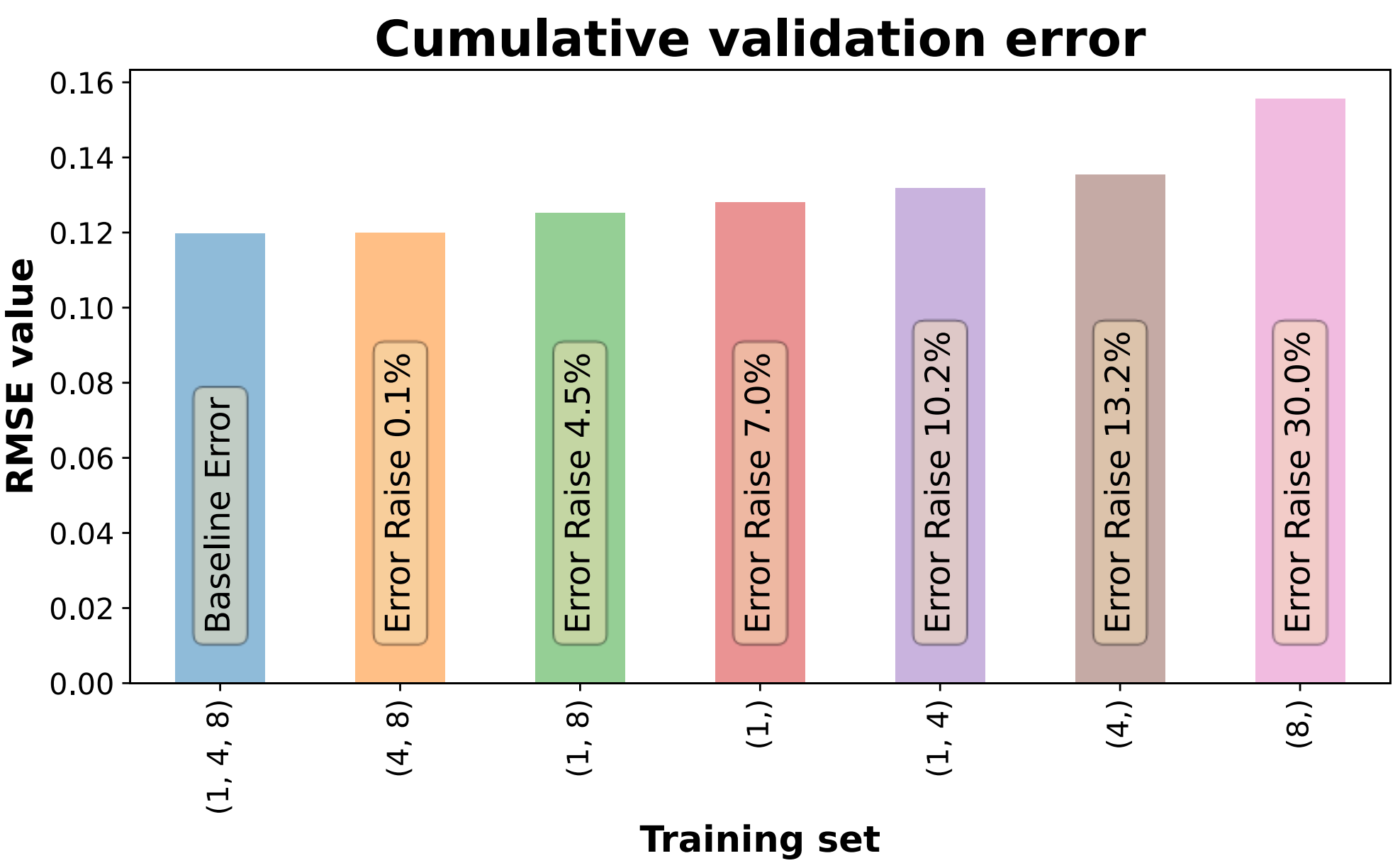
Cumulative validation error
RMSE value
0.16
0.14
0.12
0.10
0.08
0.06
0.04
0.02
0.00
Baseline Error
Error Raise 0.1%
Error Raise 4.5%
Error Raise 7.0%
Error Raise 10.2%
Error Raise 13.2%
Error Raise 30.0%
(1, 4, 8)
(4, 8)
(1, 8)
(1,)
(1, 4)
(4,)
(8,)
Training set

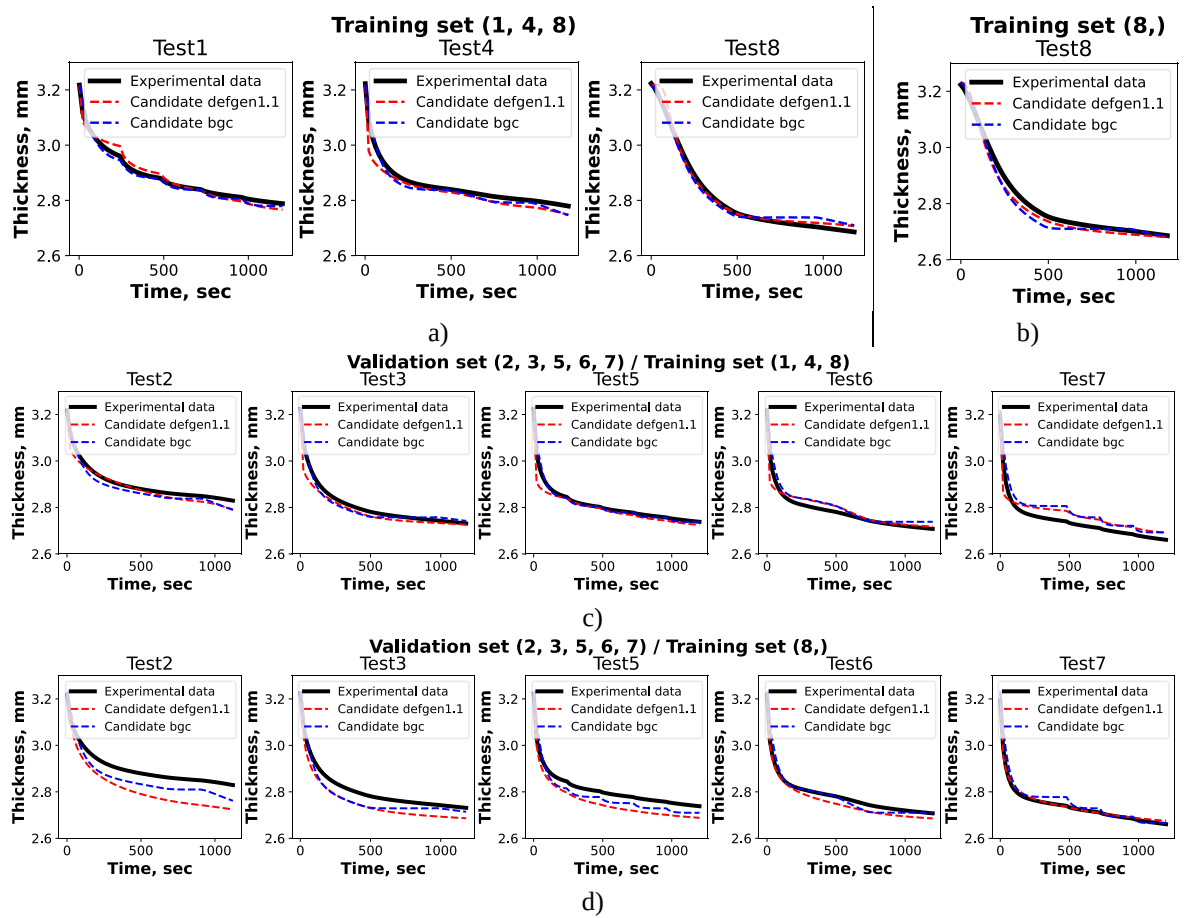
Training set (1, 4, 8)
Test1
Test4
Test8
Experimental data
Candidate defgen1.1
Candidate bgc
Thickness, mm
Time, sec
a)
Training set (8,)
Test8
b)
Validation set (2, 3, 5, 6, 7) / Training set (1, 4, 8)
Test2
Test3
Test5
Test6
Test7
c)
Validation set (2, 3, 5, 6, 7) / Training set (8,)
Test2
Test3
Test5
Test6
Test7
d)